inter•noise 96
25th Anniversary Congress – Liverpool

INCE: 38

ACTIVE CONTROL OF BROADBAND RANDOM NOISE IN RECTANGULAR ENCLOSURES

Y C Park (1) & S D Sommerfeldt (2)

(1) Micro Division, DSP Team, Samsung Electronics Co, Korea, (2) Dept of Physics & Astronomy, Brigham Young University, USA

1. Introduction

In recent studies, it has been demonstrated that a significant improvement in overall attenuation of noise signals is possible by sensing and minimizing the total energy density, rather than the squared pressure[1,2]. Energy-based control has also the advantage of overcoming the spillover problem that often leads to localized zones of silence hen controlling the measured acoustic pressure in a field. Practical versions of such systems have so far demonstrated substantial and reliable control results in the case of deterministic signals. Considering the fact that noise fields being controlled are often generated by broadband noise sources, there exists a need to also control broadband random noises.

In this study, we present numerical results that demonstrate the global attenuation of broadband noise in a three-dimensional enclosure achieved by minimizing the energy density. Analyses presented here are undertaken by designing time domain optimal filters that always satisfy the causality constraint.

This study is an extension of one-dimensional work reported previously in Ref. 3. In the one-dimensional case, it was shown that controlling energy density at a single location yields global attenuation results that were superior to controlling pressure and comparable to controlling potential energy. It was also shown that, unlike the case of controlling pressure, the energy-based control did not demonstrate any dependence on the error sensor location. In three dimensional enclosures, however, the same result is not obtained since it is generally known that the energy density in this case is a function of the measurement location. Numerical results presented here are compared with controls that one could achieve by minimizing the squared pressure and potential energy in the enclosure.

2. Optimization of Control Filters

A digital model of the optimal noise control system is schematically illustrated in Fig. 1, where subscripts $_p$, $_{vx}$, $_{vy}$, and $_{vz}$ indicate pressure, x, y, and z components of the velocity, respectively. The blocks P and H represent transfer functions of

the paths from noise source to error sensors and from control filter output to error sensors, respectively. The sampled acoustic signal detected by the sensor is equal to the sum of the primary signal, $d_i(k)$, due to the primary noise source, and the control signal due to the output of the actuator, so that

$$e_i(k) = d_i(k) + \mathbf{w}^T \mathbf{r}_i(k), \quad i = p, vx, vy, vz \tag{1}$$

where $\mathbf{w}=[w_0\ w_1\ \cdots\ w_N]^T$ is the coefficient vector of the N-th order control filter and $\mathbf{r}_i(k)=[r_{i,0}\ r_{i,1}\ \cdots\ r_{i,N}]^T$ denotes the filtered reference input vector.

The objective of the optimal controller design is to find the coefficient vector $\mathbf{w}$ minimizing a chosen performance function. The optimal coefficient vector can be obtained by using several different performance functions, such as squared pressure, energy density, and potential energy. Measuring the acoustic potential energy is very difficult to measure in practice. However, an approximate measure is often obtainable by the use of an array of acoustic pressure sensors. The three performance functions are expressed as

$$J_{SP} = E\{e_p^2(k)\} \tag{2}$$

$$J_{ED} = \frac{E\{e_p^2(k)\}}{2\rho c^2} + \frac{\rho E\{e_{vx}^2(k) + e_{vy}^2(k) + e_{vz}^2(k)\}}{2} \tag{3}$$

$$\hat{J}_{PE} = \frac{1}{4\rho c^2} E\left\{\sum_{j=1}^{N_e} e_{p,j}^2(k)\right\} \tag{4}$$

where it is assumed that an approximate measure of the potential energy is obtained using a sensor array consisting of N_e sensors.

The optimization is accomplished by finding the coefficient vectors minimizing the corresponing cost functions. The results of the optimization can be expressed as

$$\mathbf{w}_{o,SP} = -\mathbf{R}_p^{-1}(k)\mathbf{P}_p(k) \tag{5}$$

$$\mathbf{w}_{o,ED} = -\left[\mathbf{R}_p(k) + (\rho c)^2 \sum_{i=vx,vy,vz} \mathbf{R}_i(k)\right]^{-1} \left[\mathbf{P}_p(k) + (\rho c)^2 \sum_{i=vx,vy,vz} \mathbf{P}_i(k)\right] \tag{6}$$

$$\hat{\mathbf{w}}_{o,PE} = -\left[\sum_{j=1}^{N_e} \mathbf{R}_{p,j}(k)\right]^{-1} \left[\sum_{j=1}^{N_e} \mathbf{P}_{p,j}(k)\right] \tag{7}$$

where $\mathbf{R}_i(k) = E\{\mathbf{r}_i(k)\mathbf{r}_i^T(k)\}$ and $\mathbf{P}_i(k) = E\{d_i(k)\mathbf{r}_i^T(k)\}$, $i = p, vx, vy, vz$ denote autocorrelation matrices of the filtered reference input and cross correlation vectors between the primary noise input and the filtered reference input, associated with the acoustic pressure and velocity components, respectively.

3. Numerical Results

The control of the acoustic field was investigated in an enclosure having the dimensions $L_x = 1.93$, $L_y = 1.22$ and $L_z = 1.54$. A single primary and a single control source have been used for the results presented here. The primary and secondary

sources were placed at normalized positions given by $\mathbf{x}_p = (0.02, 0.02, 0.98)$, and $\mathbf{x}_s = (0.98, 0.02, 0.98)$, respectively. Impulse responses for the primary and control paths were modeled using 256-tap FIR digital filters. To this end, the modal model of the sound field[4] was used. The broadband noise signal $x(k)$ was taken to be white noise filtered through a bandpass filter with a pass band from 50 to 350 Hz, and the sampling rate was set to 1000 Hz. To simulate potential energy control, 6 pressure microphoes were placed at each of the corners of the enclosure, except the two corners occupied by the primary and control sources. The controller was then designed using Eq. 7. This approach provides a simple way of approximating potential energy control[5]. The same 6 microphones were used to test the global attenuation. The global attenuation was measured by averaging the power spectral density (PSD) of the outputs from the microphones.

Figs. 2 and 3 show the attenuation in the PSD level achieved by using each of the three control approaches, for the configurations $\mathbf{x}_e = (0.3, 0.5, 0.5)$ and $\mathbf{x}_e = (0.7, 0.5, 0.5)$, respectively. In the first configuration, the error microphone is located at a position closer to the primary source than to the control source, so that many of the primary noise components delievered to the error microphone via direct as well as reflected paths are not controllable with the causal control filter. For this reason, the squared pressure control increases the PSD level at most frequencies in this configuration. The energy density control, on the other hand, shows reasonable control results at most frequencies. In the second configuration, which is considered as a causal situation in the geometrical sense, the squared pressure control still exihibits negative attenuation at some frequencies, while the energy density control shows the results that are similar to the previous case.

Additional observations on the control effect can be obtained by looking at the impulse response of the optimal controllers. The control filters were optimized for each error sensor location, which varies from 0.02 to 0.98 in the x-axial direction. The results are shown in Fig. 4. It is clearly shown that when controlling the squared pressure, the performance of the control system is highly dependent on the error sensor location. On the other hand, the energy density control exhibits results that are relatively insensitive to error sensor location. However, it should be noted that the energy-based control is not completely independent of the error sensor location. Unlike the one-dimensional case, the energy density field in the three-dimensional enclosure is a function of the measurement location. As a result, the control filter designed to minimize the energy density at a discrete location generates attenuation results that vary some according to sensor location, as can be seen from Figs. 2, 3 and 4. However, as mentioned previously, the performance is still relatively consistent over the error sensor locations considered. When the implementation is considered in particular, this special property of the energy density control represents a significant advantage over the squared pressure control.

4. Conclusions.

Numerical results are presented to predict the performance of active noise control systems designed to control broadband noise signals in a three-dimensional enclosure. The energy-based control yielded attenuation results that are relatively insen-

sitive to the error sensor location, while the squared pressure control exhibited the performance that is highly dependent on the error sensor location.

References

1. S.D.Sommerfeldt and P.J.Nashif, *J. Acoust. Soc. Am.*, 96(1) 300-306 (1994)
2. S.D.Sommerfeldt, J.W.Parkins and Y.C.Park, *Proc. Active 95*, 477-488 (1995)
3. Y.C.Park and S.D.Sommerfeldt, *J. Acoust. Soc. Am.*, to be published.
4. P.A.Nelson and S.J.Elliott, *Active Control of Sound*, Academis Press (1994)
5. S.Sakamoto, S.Ise and H.Tachibana, *Proc. Active 95*, 549-560 (1996)

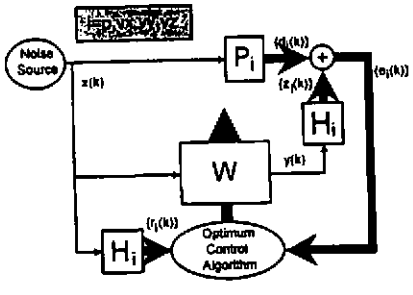

Fig.1. Digital model of ANC system.

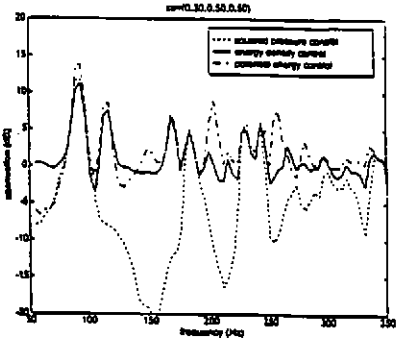

Fig.2. Attenuation results with xe=(0.3,0.5,0.5).

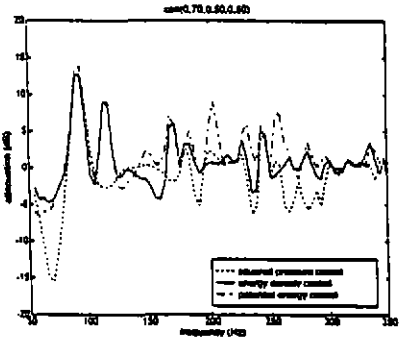

Fig.3. Attenuation results with xe=(0.7,0.5,0.5).

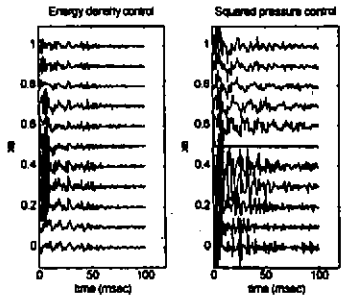

Fig.4. Control filter impulse responses.